NEUTRAL HYDROGEN NEAR THE EARTH AND IN INTERPLANETARY SPACE

V. G. KURT

Usp. Fiz. Nauk 81, 249-270 (October, 1963)

INTRODUCTION

THE opinion prevalent at the beginning of this century was that the earth's atmosphere above the tropopause (stratosphere) was stationary, without turbulent mixing. The different components of the atmosphere were therefore assumed to obey Dalton's law (the law of independent distribution of the density under isothermal conditions), the density of each component being determined by its own barometric formula

$$n_i(h) = n_i(0)\exp\left\{-\frac{\mu_i m_p g h}{kT}\right\}, \quad (1)$$

where $n_i(h)$ —concentration of the i-th component at height h, μ_i —molecular weight of the i-th component, g —acceleration due to gravity, and k, m_p, T —the Boltzmann constant, the proton mass, and the absolute temperature.

Putting $kT/\mu_i m_p g = H$, we get

$$n_i(h) = n_i(0)\exp\left\{-\frac{h}{H}\right\}, \quad (1')$$

where H is the height of the homogeneous atmosphere customarily referred to as the height scale. It can be shown [1] that when the dependence of g on the height is taken into account, we have at high altitudes

$$n_i(h) = n_i(0)\left(\frac{R_E}{R_E+h}\right)^2\exp\left\{-\left(\frac{h}{R_E+h}\right)\left(\frac{\mu_i m_p g_0 R_E}{kT}-2\right)\right\}, \quad (2)$$

where R_E —radius of the earth and g_0 —acceleration due to gravity at sea level. Accordingly, it seemed obvious that above approximately 75 km the main atmospheric component was molecular hydrogen. These notions were essentially developed by Jeans [2-4], who obtained a relatively simple formula for the flux of hydrogen atoms leaving the earth, i.e., with velocity larger than parabolic at the dissipation level. This flux can be obtained by integrating the Maxwellian distribution

$$F_d = \frac{n(H/h_d)}{4}\int_{v_\infty(h_d)}^{\infty} v f(v)\, dv. \quad (3)$$

Integrating, we get

$$F_d = \frac{\bar{v}(h_d)\, n_\Sigma(h=0)\, Y e^{-Y}}{\sqrt{6\pi}}\left[\frac{R_E+h_d}{R_E}\left(1+\frac{R_E+h_d}{YR_E}\right)\right], \quad (4)$$

where

$$Y = \frac{3v_\infty^2(h=0)}{2\bar{v}^2}. \quad (4')$$

Here $\bar{v}(h_d)$ —mean square of velocity at the dissipation level; $n_\Sigma(h=0)$ —the atmospheric density which would exist at the earth's surface if the atmosphere at all altitudes were isothermal with a temperature corresponding to the dissipation rate at the earth's surface $v_\infty(h=0)$: h_d is the height of the dissipation level.

In 1919, Chapman [5] showed that mixing in the atmosphere can extend considerably above the tropopause, and in this case the fraction of the hydrogen should be constant and quite small. Until 1950 it was assumed that the role of hydrogen was small, but the situation changed noticeably since. Within approximately 10—15 years a tremendous number of papers were published on a great variety of aspects of this problem. It should be stated that the main impetus for a restudy of this problem were the investigations of Meinel [6,7], V. I. Krasovskiĭ [8], and I. S. Shklovskiĭ [9], who demonstrated beyond any doubt that the glow of the night sky in the near infrared is connected with the hydroxyl rotational-vibrational spectrum. This suggested to Bates and Nicolet the need for studying the photochemical reactions that lead to the appearance of the OH molecules, and consequently of the H_2O and H_2 molecules and of the hydrogen atoms.

Being the lightest neutral particle, hydrogen, of course, readily diffuses upward. Even the electrons acquire as a result of the electrostatic attraction to the ions a height distribution corresponding to half the molecular weight of the neutral particle from which this ion has been formed, i.e., at least seven times the molecular weight of hydrogen.

We thus return, as is frequently the case in science, to the earlier views concerning the major role of hydrogen in the upper layers of the atmosphere. To be sure, the height at which the fraction of the hydrogen becomes appreciable is not 75 but 2000 km, but this is caused, first, only by the fact that the mixing in the atmosphere extends to higher altitudes, at least to 100 km, and second by the different reactions into which hydrogen enters. Rocket astronomy has made possible many optical experiments confirming this point of view. These experiments are at present probably the main source of information on the composition of the upper layers of the earth's atmosphere and interplanetary space.

During the last five years we have also learned the spectral composition of the sun's ionizing radiation (see the reviews [10] and [11] on this subject). In conjunction with the measurements of the electron density in the upper ionosphere and in the interplanetary space,

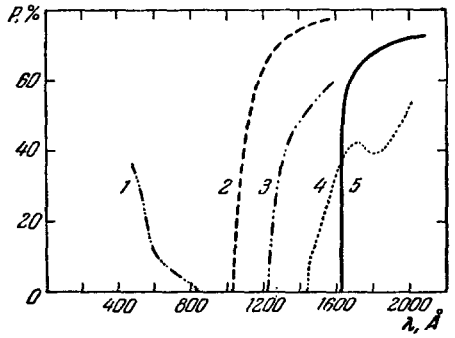

FIG. 1. Transmission of some materials in the ultraviolet region of the spectrum. 1–aluminum, 0.1 μ thick; 2–lithium fluoride; 3–calcium fluoride; 4–corundum; 5–crystalline quartz.

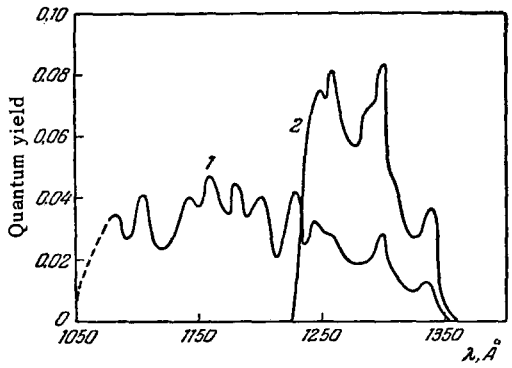

FIG. 2. Sensitivity curves of two photon counters with windows of lithium fluoride and calcium fluoride (fluorite).

it is now possible to calculate the ionization of the hydrogen. Finally, new instruments, neutral composition mass spectrometers, can in principle measure directly the concentrations of the neutral hydrogen, although so far only in the lower layers of the atmosphere. Rocket investigations of the chemical composition of the atmosphere, and also measurements of the neutral-component density, have permitted a closer examination of the origin of hydrogen in the earth's upper atmosphere.

In the first section we report the experimental results obtained mainly with artificial satellites and rockets, while the following sections will present a theoretical analysis of these observations.

1. EXPERIMENTAL PROOF OF THE EXISTENCE OF HYDROGEN IN THE UPPER ATMOSPHERE OR IN INTERPLANETARY SPACE

Rocket measurements in the ultraviolet region of the spectrum have made possible observation of the solar L_α radiation scattered by the hydrogen atoms. To this end, photon counters sensitive to the narrow region of the spectrum near the L_α line (1215 Å) have been developed [12]. The operating mechanism of such a counter is based on the photoionization of nitrogen oxide, with a distinct threshold at $\lambda = 1350$ Å that determines the long-wave sensitivity limit of the counter. The short-wave sensitivity limit depends on the transmissivity of the instrument window material. Transmission curves for several substances used in ultraviolet-radiation research are shown in Fig. 1. By varying the gas in the counter it is also possible to shift the long-wave limit of the instrument. In addition to the sensitivity in the ultraviolet, which is of interest to us, the quantum counters also have a sensitivity, of the order of 10^{-5} of maximum, in the long-wave part of the spectrum, beyond the limit of the photoionization threshold, due to photoelectronic emission from the counter cathode. The spectral region of interest near the L_α line is investigated either with the aid of the photon counters described above, or with the aid of ionization chambers. In the latter case it becomes necessary to employ sensitive dc amplifiers, whereas more reliable devices (counting-rate meter or a circuit that counts each pulse) can be used with a counter. The dark current of a counter filled with NO can be reduced to the several pulses per second due exclusively to cosmic rays. The sensitivity of counters made with windows of LiF and CaF_2, used at the Naval Research Laboratory [13], is shown in Fig. 2. A quantum counter with calcium-fluoride window is insensitive to L_α radiation, but according to Friedman [14] the short-wave transmission limit of CaF_2 depends strongly on the temperature, which may cause errors in the comparison of counter readings.

The first night sky glow in the L_α line was observed in a rocket experiment performed by the Friedman group (USA) [13,15] in November 1955, using an Aerobee research rocket launched at night from the White Sands proving grounds. Two narrow-band counters with LiF and CaF_2 windows and one counter with greater bandwidth were mounted on the rocket, perpendicular to its axis. The narrow-band counters had collimators with a subtended angle 20° and a window area 0.3 cm^2. The broadband counter had a sensitivity of several per cent up to 1470 Å. Both types had quantum yields $\sim 10^{-6}$ at 1600 Å, 10^{-7} at 1800 Å and 10^{-8} at 2200 Å. The broadband counter had no collimator and subtended a larger field of view. The rocket also carried a collimator-equipped photomultiplier for the registration of the night sky glow in the visible region, making it possible to determine, in conjunction with the magnetometer readings, the orientation of the rocket in flight. The broadband quantum counter started operation at 23 km and reached saturation at 33 km. Its count decreased, starting with 69 km and again reached full scale at 75 km. The narrow-band photon counter with the LiF window started operating at 75 km and saturated at 79 km. Readings were obtained with the counter pointing both upward and downward. The counter with CaF_2 detected no radiation when it registered only the presence of stellar objects and also the Milky Way belt. The authors then estimated the L_α brightness of the sky at 5×10^{-5} erg/cm^2 sec-sr at 80 km and 3×10^{-4}

erg/cm^2 sec-sr for the region above the atmospheric absorption. The value obtained for the absorption coefficient agreed well with the coefficient of absorption of L_α radiation by molecular oxygen. Thus, all the observational data have favored the hypothesis that the ultraviolet emission is connected with the scattering of solar L_α quanta by neutral hydrogen.

The next experiment by the same authors demonstrated this conclusively [16-19]. The rocket was launched on 28 March 1957 to a height of 146 km. The radiation receiver was an ionization chamber with a collimator providing a field of view ~ 32°, and the sky was scanned as the rocket turned. At an altitude of 75 km radiation above the rocket was observed from the entire sky, and a glow from below the rocket appeared also starting with 85 km. Both fluxes increased up to 120 km, above which they remained constant to the top of the trajectory. The data obtained were used to plot the isophots from 130 to 146 km shown in Fig. 3. The isophots are almost concentric circles with a minimum at the center.* The latter is shifted from the antisolar point by 8°. The range of brightness variation is quite narrow, $(3.6-2.7) \times 10^{-3}$ erg/cm^2 sec-sr. According to these observations the albedo is very high and amounts to 42%, whereas the daytime albedo of the atmosphere is at most less than 2%.

New data were obtained in 1960 by lifting the "Javelin" rocket to 1120 km. The radiation receiver was an ionization chamber mounted perpendicular to the rocket axis [20]. The field of view of the chamber was 31° 44′ at the center of the window and increased to 44° 10′ at the edge. The launching was on 14 January from the Wallops Island (Virginia) at 13:15 GMT. It should be noted that although this experiment could have answered many questions, apparatus malfunctioning greatly reduced its value. First, the orientation of the rocket was known only approximately, in spite of its being equipped with a magnetometer. During the flight, the rocket apparently rotated at 2 rps and precessed with a period of 4.5 seconds about an axis inclined 44°. The antisolar point was approximately 15° south of the zenith. An examination of the telemetered records has shown that the curve has a double minimum, which depends on whether the chamber passes through the nadir or through the antisolar point. The particularly deep minimum is apparently connected with the vertical scanning of the photometer. Another feature were very large readings observed approximately every 0.5 sec and connected, in the authors' opinion, with the aurora. It is obvious that for a tentative analysis we can put

$$\frac{dI_z}{dh} = (I_z - I)\, n\,(\mathrm{H}/h)\,\bar{\sigma}, \qquad (5)$$

where I_Z — intensity at the zenith, I — intensity averaged over the period of revolution, and $\bar{\sigma}$ — average scattering coefficient.

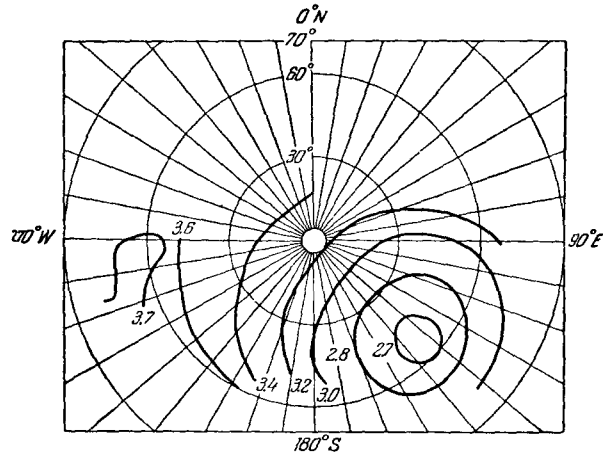

FIG. 3. L_α isophots of the night sky in units of 10^{-3} erg/cm^2 sec-sr.

The intensity at the nadir (the minimum reading during the period), which we denote by I_n, should evidently not depend on the altitude. This statement follows from the foregoing experiment. Setting I_n constant, the authors introduce corrections to I and I_Z, assuming that the errors in the latter entail an increase in all the readings, starting with approximately 800 km (300 seconds following the launching). This rather arbitrary operation makes I_Z a quantity that decreases monotonically with increasing altitude (approximately 15% on going from 500 to 1100 km.) Choosing for the average resonant scattering coefficient $\bar{\sigma}$ a value 1.7×10^{-13} cm^2 at T = 1250°K, equal to the scattering coefficient at the center of the line, we obtain for n(H)/h lower limits 1.3×10^5 cm^{-3} at 800 km and 0.8×10^5 cm^{-3} at 1100 km.

The albedo calculated from these measurements for 500 km, where the apparatus functioned normally, is approximately 65%, and linear extrapolation to 200 km yields 58%, as against 42% in [16]. However, this discrepancy can be readily attributed to the shift of the null of the instrument, the sensitivity of which could not be calibrated in flight; in addition, linear extrapolation down to 300 km can hardly be justified. The main deduction concerning the high value of the nighttime albedo can be regarded as confirmed. The average intensity of the night sky glow is 1.2×10^{-3} erg/cm^2 sec-sr, which also agrees well in order of magnitude with the abovementioned experiment.

There is no doubt that such experiments must be repeated up to distances of the order of $10\,R_E$. With apparatus having low sensitivity to radiation with $\lambda > 1350$ Å, and also with all possible measures taken to reduce the scattered light, it would also be possible to perform a daytime experiment at altitudes above 200 km. In fact, Rayleigh scattering at 100 km yields ~ 10^{-2} erg/cm^2 sec-sr in the entire visible region, which results in a reading 10^2—10^3 times as small as the L_α glow of the sky for an instrument sensitivity ~ 10^{-5}

*The bending of the isophots to the west at z = 60° is due to a region in Orion where a group of hot stars and nebulae is located.

outside the operating band. The visible and solar L_α radiation scattered in the instrument can be attenuated by 3—4 orders of magnitude, which is sufficient for observation of the daytime L_α emission.*

It was necessary to verify whether the radiation in the 1050—1230 Å band is L_α emission or whether it is connected even partially with the Lyman-Birge-Hopfield N_2 bands or the O_2 bands which, according to Fastie's estimates [21], could be registered by the apparatus.

To this end, an "Aerobee" rocket was raised twice in 1961 (April 17 and October 31) to 177 and 212 km [22]. The rocket carried in both cases spectrographs with bent diffraction gratings (F = 400 mm, 600 lines/mm first order). The spectrograph had a 67° field 330 Å/mm dispersion, and 6 Å resolution. The exposure was 5 minutes, and in the first launching the rocket rotated in disorderly fashion during this time. In the second case, the rocket rotated about a longitudinal axis and the spectrograph axis was inclined 7° downward. In both cases no radiation other than the L_α emission, with intensity exceeding 0.1 of the L_α intensity, i.e., 4×10^{-4} erg/cm² sec-sr, was observed in the spectral region 1150—1700 Å. The continuous spectrum in this region was in any case weaker than 2×10^{-5} erg/cm² sec-sr-Å.

Reproductions of the spectrograms obtained in this experiment are shown in Fig. 4.

For a detailed study of the nature of the night glow of the atmosphere, it is necessary to obtain a spectrum with a resolution of 0.01 Å, which is so far unattainable. However, some information on the line width can be obtained also by a filter technique. The filter employed was a cuvette with molecular hydrogen and two lithium-fluoride windows [23]. The H_2 was dissociated by heating a tungsten filament, and a quantity of atomic hydrogen sufficient for the absorption of the L_α radiation was produced. The radiation receiver was an ionization chamber. The half-width of the absorption line measured in the laboratory was 0.08 ± 0.02 Å. The instrument had 6° a field of view and was raised simultaneously with a spectrograph on April 17, 1961, the sun's depression angle being 25°. A program device turned the filaments on periodically. A photomultiplier with a 3.5° field was connected in parallel with the described instrument, and its readings were used to calculate the orientation of the rocket.

The result of this highly important experiment can be briefly summarized as follows:

(1) With the instrument facing the earth and the filaments turned off, the albedo was 40%, in perfect agreement with the experiment of 1957 [16].

(2) When the filaments were turned on, the reading dropped to zero (within 2%) when the photometer faced downward and (3) to 15% when the photometer faced upward.

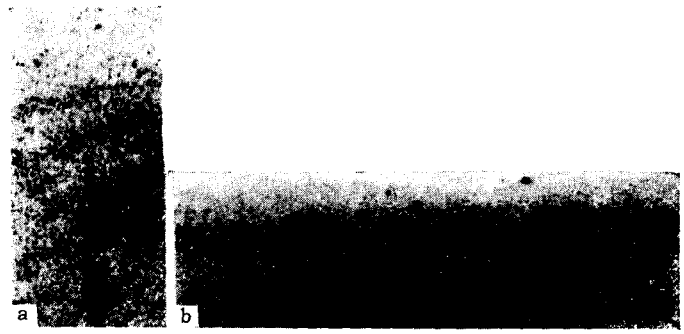

FIG. 4. Spectograms of the night sky glow, showing the L_α line, the only emission line in the 1150 – 1700 Å region.

The authors discuss several explanations of this effect.

It can be regarded as established [22] that there is no emission other than L_α in the sensitivity range of the photometer. It is most probable that some of the hydrogen has a temperature ≥ 7000°K, which is sufficient for part of the scattered radiation to pass through the hydrogen filter. A stationary interplanetary gas at rest relative to the earth would result in large fluctuations of the residual radiation, owing to the Doppler effect connected with the orbital motion of the earth, but this was not observed.

A second no less important way of observing neutral hydrogen is based on a study of the profile of the solar L_α emission line, which should have an absorption core at the center. It is obvious that the width of this core will be ~ 0.02 Å for $T = 3 \times 10^4$ °K. The existence of such a center was predicted in 1955 as a result of an already mentioned investigation of the night sky glow [13]. G. M. Nikol'skiĭ [24] made an analogous calculation for the case of localization of hydrogen in interplanetary space at high temperature and density.*

A profile with the necessary resolution was obtained by Purcell and Tousey [25], who used a double-dispersion spectrograph with bent grating (R = 50 cm, 1200 lines/mm). The first grating, operating in the first order, produced an image of the sun in a line on the spectrograph slot, so that the scattered light was sufficiently small. The second grating operated in the thirteenth order and the dispersion was 0.4 Å/mm. The overall system was stigmatic and the quality of the spectrograms was splendid. The half-width of the instrumental profile was 0.3 Å by laboratory measurements. The spectrograph was raised on July 21, 1959 and April 18, 1960, but only the results of the first launching were published. The rocket reached 198 km at a sun zenith angle 69°, the exposure ranging from 4 to 120 seconds at altitudes from 92 km upward. The L_α line is very broad and has wings extending to 1 Å and further on both sides of the center. At the center of the line there is a broad but shallow absorbing core, as well as a predicted narrow deep core. No notice-

*Note added in proof. At the sixth COSPAR conference in Warsaw (June, 1963), Fastie and Donahue presented new day- and nighttime experimental results obtained with rockets raised to 220 km. Radiation in the L_α line and in λ1302 Å of OI was registered.

*A modern estimate of the density of the hydrogen atoms in interplanetary space yields ~ 0.03 cm^{-3}, which is one-hundredth of the value assumed by G. M. Nikol'skiĭ.

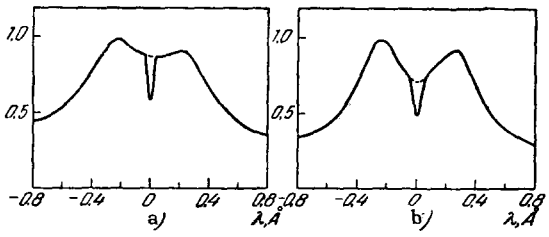

FIG. 5. Profile of L_α line, obtained July 21, 1959. a) near the center of the sun's disc; b) near the edge.

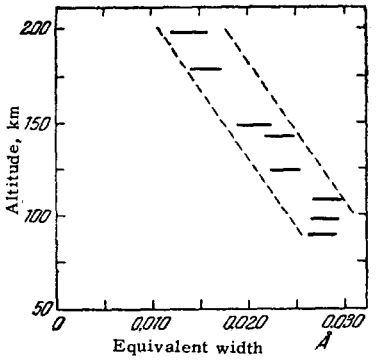

FIG. 6. Dependence of W on the altitude.

able Doppler shift was observed (Fig. 5).

The broad dip at the center of the line is well explained by the theory of line production in the chromosphere with allowance for incoherent scattering, developed by Thomas N. Jeffrey[27] and by Morton and Waiding[28]. The width of the absorption core of interest to us corresponds to a temperature in the interval 800—2100°K, and its equivalent width W decreases monotonically with altitude from 0.028 Å for 97 km to 0.014 Å for 197 km. For a vertical column, assuming that the hydrogen is located for the most part near the earth, the quantity

$$N(\mathrm{H}/h)=\int_h^\infty n(\mathrm{H}/h)\,dh$$

is equal to 2×10^{12} cm^{-2} at h = 197 km. A plot of W(h) is shown in Fig. 6.

The authors propose to employ in the future a spectrograph with an echelle (73 lines/mm) operating in the 200th order. The resolution of this instrument will be one order of magnitude higher than that of a spectrograph with a grating in the 13th order.

Among the indirect experiments connected with the presence of hydrogen, notice should be taken of the emission of the night sky in the H_α line, discovered by V. S. Prokudina and first interpreted by I. S. Shklovskiĭ[29] as being the result of "reprocessing" of solar L_β quanta. This causes re-radiation of H_α and L_α or L_β photons, in amounts having the same ratio as the Einstein transition probabilities, i.e., 1 : 1.25 for an optically thin layer. According to the latest data, the intensity of the L_β line is 0.03 erg/cm^2 sec, which is approximately 100 times as small as the L_α intensity. In this case, for a 45° depression of the sun below the horizon, corresponding to the experimental data[16] (see Fig. 3), the brightness in the H_α line for the zenith should be approximately 10^6 photons/cm^2 sec-sr or 10 R.* The observations of Prokudina[30] and Fishkova[31] lead apparently to the same value. It must be noted that the hydrogen corona of the earth is transparent to H_α radiation. Therefore, an H_α-line sky map would help obtain the distribution of the hydrogen atoms as a function of the distance. Analogous observations were carried out in Norway by Kvifte[32], who obtained approximately 6 R for the upper intensity limit. Fishkova's observations, which cover several years, lead to the conclusion that the brightness has a minimum (a factor of approximately 3) in the antisolar point. These observations are particularly important because the spectrograph was under pointing control during the exposure. Shcheglov[26] used a Fabry-Perot etalon in conjunction with an electron-optical converter. Such a procedure ensured high sensitivity and good angular resolution. Brightness variations were registered at the world pole (at an average brightness of 10^{-5} erg/cm^2 sec-sr) and the presence of a minimum at the antisolar point was confirmed. The width of the instrumental profile was only 0.3 Å, whereas the H_α line in galactic gas nebulae is in many cases broader. This has made it possible to separate reliably the geocoronal line from the galactic background.

Notice should be taken of the work by Ingham[33], who obtained two spectra with narrow H_α line during an expedition in Bolivia. Both spectra were obtained in the first and second halves of the night with a stationary spectrograph (z = 82°) and were calibrated against a standard lamp. The H_α line intensities obtained (10.8 and 8.1 R) were corrected for the influence of the galactic background, yielding values 6.0 and 4.2 R.

Further, measurements of the density of the upper atmosphere at altitudes exceeding 1000 km, by determining the drag of the "Echo 1" satellites, yielded the density and height of the homogeneous atmosphere up to 1700 km[34]. Assuming that the atmosphere above 1500 km consists of helium and hydrogen, we obtain for n(H/h) a value 8×10^5 cm^{-3}. It will be made clear below that this value is at least one order of magnitude too high.

Finally, measurements of the electron density at high altitudes (see, for example, [35]) have shown that starting with 1500—2000 km the gradient of the electron density decreases sharply. This is naturally explained by the transition from an oxygen-nitrogen plasma to a helium-hydrogen plasma.

Thus, the aggregate of the observed data leads to the following conclusions, which must be theoretically explained:

*1 Rayleigh = 1R = 10^6 photons/cm^2 sec · 4π.

1) The nighttime albedo of the atmosphere in the L_α line is ~ 40%, while the daytime albedo is < 2%.

2) The distribution of the brightness in the L_α line over the sky corresponds at night to Fig. 3, with the minimum shifted from the antisolar point by ~ 8°.

3) During the day N(H/h) above the 120 km level is approximately 2×10^{12} cm^{-2} and the equivalent width of the absorption core in the middle of the L_α line varies with altitude in accordance with Fig. 6.

4) Approximately 15% of the radiation emitted upward (at a height of 177 km) has an L_α line width corresponding to $T \geq 7 \times 10^3$ °K.

2. DISTRIBUTION OF HYDROGEN IN THE EARTH'S UPPER ATMOSPHERE

Interest in the photochemical reactions occurring in an oxygen-hydrogen atmosphere in the presence of water vapor has increased following the observation of the hydroxyl molecule bands in the spectrum of the night sky glow. At sea level, the water content is exceedingly small, 2.6×10^{-2} cm^{-3} at the equator and 9×10^{-3} and 2.2×10^{-3} cm^{-3} at 50 and 70°N respectively [36]. With increasing altitude and decreasing temperature, the concentration of water vapor decreases to 10^{-5} cm^{-3} at 200°K. Naturally, starting with a certain altitude, the water vapor becomes dissociated by the ultraviolet radiation from the sun, with a wavelength shorter than 2400 Å, which penetrates to 50 km [37]. The corresponding reaction is $H_2O + h\nu \rightarrow OH + H$. The effective cross section of this process is at first extremely small (7.5×10^{-23} cm^2 at λ 2000 Å [38]) and increases to 4×10^{-18} cm^2 at λ 1680 Å. However, owing to the presence of a strong Schumann-Runge continuum [39], the radiation is absorbed by the oxygen molecules below 100 km. The predissociation process is apparently also insignificant.

Thus, it is necessary to consider all the conceivable reactions between H, OH, O, O_2, and O_3. This was done by Bates and Nicolet [40], who investigated the equilibrium distribution of the components in a hydrogen-oxygen atmosphere.

Atomic hydrogen can be released, in addition to photodissociation of H_2O, also in the following reactions:

$$\begin{aligned} OH + O &\rightarrow H + O_2, \\ OH + h\nu &\rightarrow O + H, \\ HO_2 + h\nu &\rightarrow H + O_2, \\ H_2 + OH &\rightarrow H_2O + H, \\ H_2 + O &\rightarrow OH + H. \end{aligned}$$

The hydrogen atoms disappear as a result of the reactions with O, O_2, O_3, OH, and HO_2, during the course of which the compounds OH, HO_2, H_2, O, and H_2 are again produced. Some of the reactions occur with a third particle participating. Substituting the reaction rates in the stationary equations, we can calculate the sought concentrations, which are plotted in Fig. 7. Above 100 km, all the components with the exception of O and H have negligible concentrations. At high altitudes the principal mechanism for the transport of hydrogen atoms is diffusion, and the flux of outgoing atoms at an altitude of 100 km is approximately equal to the concentration at this altitude, i.e., n(H/100 km) ~ 10^8 cm^{-3}. This entire flux is dissipated from the earth's atmosphere, as the result of which the atmosphere can become enriched with oxygen to an extent of 10^{24} atoms/cm^2 over a time of ~ 10^9 years. The distribution of the hydrogen in the height interval 120—550 km will be considered later. Starting with approximately 500 km, the role of the collisions becomes insignificant.

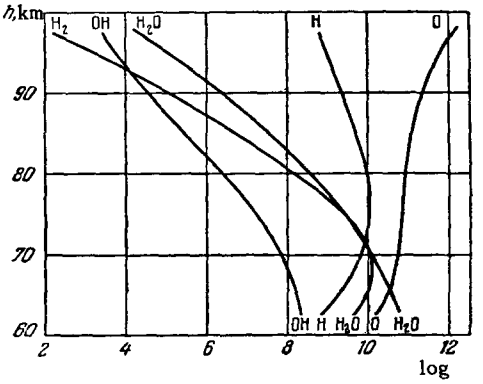

FIG. 7. Concentration of the reaction products in an oxygen-hydrogen atmosphere.

The problem of the distribution of the neutral atoms of hydrogen in the exosphere was first considered by Jeans [3]. Dissipation of hydrogen from the earth's atmosphere was subsequently treated in many papers, of which we shall consider only two, by Johnson and Fish [41] and by Öpik and Singer [42-44].

According to [41], all the orbits of the atoms at a certain level can be divided into four groups:

1. Elliptic, with perigee below the considered level.
2. Elliptic, with perigee above this level.
3. Hyperbolic: (a) Trajectories of non-returning atoms with radial velocity component > 0 and perigee below the specified level; (b) with radial component of velocity < 0 and perigee also below the level; in this case the atoms will return to the exosphere.
4. Hyperbolic trajectories, lying entirely below the considered sphere, with unlimited radial velocity component and perigee below the given level.

For a sufficiently remote point, the atoms with parabolic trajectories can be completely neglected. From the total distribution we can also exclude groups (3b) and (4), the fraction ξ of which varies with altitude from zero at the base of the exosphere to unity at infinity. Its value is 10, 40, and 55% respectively for $R = 2R_E$, $4R_E$, and $6R_E$ respectively. The altitude distribution of the atoms can then be obtained from the formula

Table I

$\frac{R}{R_E+h_d}$	n (H/h)			$\frac{R}{R_E+h_d}$	n (H/h)		
	T= =1250° K	T= =1500° K	T= =1800° K		T= =1250° K	T= =1500° K	T= =1800° K
1.000	100.0	100.0	100.0	2.000	4.1	5.7	7.5
1.111	54.9	58.9	62.2	3.333	0.96	1.11	2.2
1.250	30.3	34.8	38.7	5.000	0.03	0.35	0.70

$$n(\mathrm{H}/R) = 4(1-\xi)F_d\left[\int_{v_\infty(R)}^{\infty} v\left(\frac{m}{2\pi kT}\right)^{3/2}\exp\left\{-\frac{mv^2}{2kT}\right\}dv\right]^{-1}\left(\frac{R_d}{R}\right), \quad (6)$$

where F_d is the flux of dissipating particles at the dissipation level, $v_\infty(R)$ is the parabolic velocity at the level R, and R_d is the distance from the center of the earth to the dissipation level. Assuming, according to Bates and Nicolet [40], that $F_d = 10^8$ cm^{-2} sec^{-1}, we can calculate n(H/R) (Fig. 8). The value assumed for T in [41] is 1250°K, which is apparently somewhat underestimated.

Opik and Singer obtained the density variation by starting from other assumptions. They took into account only two types of orbits: parabolic, returning, which give twice the contribution to the total value of the density, and hyperbolic.* Particles with orbits of the satellite type constitute a small fraction of the total number of dissipating hydrogen atoms. Results of the calculations are given for different temperatures in Table I.

Below the dissipation zone, the hydrogen should apparently have a distribution obeying the diffusion-equilibrium equation [45]

$$n(\mathrm{H}/h) = n(\mathrm{H}/h_0)\left\{\frac{T(h_0)}{T(h)}\right\}^{1-\frac{\mu(H)}{\mu(0)}-\alpha}\left\{\frac{n(\mathrm{O}/h)}{n(\mathrm{O}/h_0)}\right\}^{\frac{\mu(H)}{\mu(0)}}, \quad (7)$$

where α is the thermal diffusion factor equal approximately to 0.25 [46].

However, attempts to "unify" the three regions (zone of total mixing, diffusion equilibrium, and dissipation) were unsuccessful. The point is that Eq. (5) gives too slow a decrease in density, making the density at the altitude $h = h_d$ quite appreciable. The quantity $N(H/h_d)$ is equal to $2.5 \times 10^8\, n(H/h_d)$ for the exosphere model of Opik and Singer or $0.8 \times 10^8\, n(H/h_d)$ for the Johnson-Fish distribution. Naturally, in this case the number of hydrogen atoms below 200 km was approximately 10% of the total number in the column above 100 km. Then the dependence of the equivalent width of the core of L_α line on the altitude has too small a slope in the altitude region 100—200 km, i.e., where the observations of Purcell and Tousey were made.

*There is a misprint in the first of the cited papers by Opik and Singer: the integrand in the expression for the density should contain v^3 and not v^2.

It was necessary to reduce the contribution of the exosphere to N(H/100 km), and this was done by Bates and Patterson [47], who took into account the effect of dissipation and the distribution of the hydrogen in the lower layers, i.e., in the thermosphere. The equation for the altitude variation of the density in the thermosphere is of the form

$$\frac{dn(\mathrm{H}/h)}{dh} = n(\mathrm{H}/h)\left\{\frac{1}{H}+[1+\alpha(H)]\frac{d\log T(h)}{dh}-\frac{F(H)}{D(\mathrm{H}/h)}\right\}, \quad (8)$$

where F(H) is the flux of particles dissipating in the exosphere, D(H/h) is the diffusion coefficient for hydrogen at altitude h, and H is the height of the homogeneous atmosphere for hydrogen at altitude h. In turn, we have

$$F(H) = B(H)\, n(\mathrm{H}/h_d),$$

where B(H) is the "velocity" of the dissipating atoms [46] with values 8.2×10^2, 3.1×10^3, $7 \times 4 \times 10^3$ and 2.2×10^4 cm/sec for T = 10^3, 1.25×10^3, 1.5×10^3 and 2.00×10^3 °K, respectively. The diffusion coefficient is equal to

$$\frac{2.1\cdot 10^{18}\sqrt{T(h)}}{n_\Sigma(h)},$$

where n_Σ is the total density. Integrating (6) "downward" from h_d to 100 km, we obtain the values of n(H/h), and consequently of N(H/h), listed in Table II.

For comparison we give the value $\bar{n}$(H/120 km) calculated simply from Eq. (7), i.e., without account of the flux of dissipating particles.

To obtain the data listed in Table II it is necessary to know T(h) and n_Σ(h). Bates and Patterson used the calculations of the density of the atmosphere made

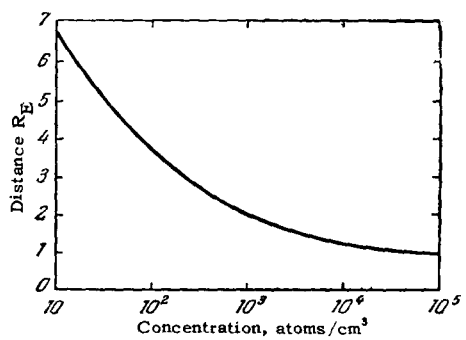

FIG. 8. Hydrogen density according to the exosphere model of Johnson and Fish.

Table II

h, km	$T(\infty)=1000°$ K		$T(\infty)=1250°$ K		$T(\infty)=1500°$ K		$T(\infty)=2000°$ K	
	n	$N\cdot10^{-12}$	n	$N\cdot10^{-12}$	n	N	n	N
100	$3.6\cdot10^6$	4,2	$8.4\cdot10^6$	8,2	$2.6\cdot10^7$	$2,1\cdot10^{13}$	$7.4\cdot10^7$	$5.5\cdot10^{13}$
110	$6.8\cdot10^5$	2,4	$1,6\cdot10^6$	3.7	$5.0\cdot10^6$	$7.5\cdot10^{12}$	$1,4\cdot10^7$	$1,8\cdot10^{13}$
120	$2.0\cdot10^5$	2.0	$4.7\cdot10^5$	2.8	$1.5\cdot10^6$	$4,7\cdot10^{12}$	$4.2\cdot10^6$	$9.8\cdot10^{12}$
130	$9.3\cdot10^4$	1.9	$2.2\cdot10^5$	2,5	$6.4\cdot10^5$	$3,7\cdot10^{12}$	$1.8\cdot10^6$	$6.9\cdot10^{12}$
140	$5.7\cdot10^4$	1,8	$1.3\cdot10^5$	2.4	$3.5\cdot10^5$	$3.2\cdot10^{12}$	$9.6\cdot10^5$	$5.6\cdot10^{12}$
160	$3.2\cdot10^4$	1.7	$6.5\cdot10^4$	2.2	$1.5\cdot10^5$	$2.8\cdot10^{12}$	$4.1\cdot10^5$	$4.3\cdot10^{12}$
180	$2.3\cdot10^4$	1,6	$4.1\cdot10^4$	2,1	$8.8\cdot10^4$	$2.6\cdot10^{12}$	$2.3\cdot10^5$	$3.8\cdot10^{12}$
200	$1.8\cdot10^4$	1.6	$2,9\cdot10^4$	2.0	$5.6\cdot10^4$	$2.4\cdot10^{12}$	$1.4\cdot10^5$	$3.4\cdot10^{12}$
250	$1.4\cdot10^4$	1,5	$1.8\cdot10^4$	1,9	$2.8\cdot10^4$	$2.2\cdot10^{12}$	$6.0\cdot10^4$	$2.9\cdot10^{12}$
300	$1.3\cdot10^4$	1.5	$1.4\cdot10^4$	1.8	$1.8\cdot10^4$	$2.1\cdot10^{12}$	$3.3\cdot10^4$	$2.7\cdot10^{12}$
350	$1.2\cdot10^4$	1.4	$1.2\cdot10^4$	1.7	$1.4\cdot10^4$	$2.0\cdot10^{12}$	$2.1\cdot10^4$	$2.6\cdot10^{12}$
400	$1.1\cdot10^4$	1.4	$1.1\cdot10^4$	1.7	$1.2\cdot10^4$	$2.0\cdot10^{12}$	$1.5\cdot10^4$	$2.5\cdot10^{12}$
450	$1.0\cdot10^4$	1,3	$1.0\cdot10^4$	1.6	$1.1\cdot10^4$	$1.9\cdot10^{12}$	$1.2\cdot10^4$	$2.4\cdot10^{12}$
500	$1.0\cdot10^4$	1.3	$1.0\cdot10^4$	1.6	$1.0\cdot10^4$	$1.9\cdot10^{12}$	$1.0\cdot10^4$	$2.3\cdot10^{12}$
120	$\tilde{n}=3.2\cdot10^4$		$\tilde{n}=3.5\cdot10^4$		$\tilde{n}=3.9\cdot10^4$		$\tilde{n}=4.6\cdot10^4$	

by King-Hele and Walker[49] on the basis of a study of the variation of artificial-satellite orbits during 1958—1960 (see the appendix). The assumption was that diffusion equilibrium sets in above 120 km and that for this altitude

$$n(N_2/120\text{ km}) = 4.4\cdot10^{11}\text{ cm}^{-3},$$
$$n(O_2/120\text{ km}) = 8.8\cdot10^{10}\text{ cm}^{-3},$$
$$n(O/120\text{ km}) = 3.4\cdot10^{10}\text{ cm}^{-3},$$
$$T(120\text{ km}) = 380°K,$$
$$\left.\frac{dT}{dh}\right|_{h=120\text{ km}} = 20\ °K/km$$

For $h > h_d$, Bates and Patterson used the ballistic model of Opik and Singer. It must be noted that all the calculation results depend strongly on the assumed limiting value of the exosphere temperature $T(\infty)$.

An absolute evaluation can be made by using the data of Purcell and Tousey[25]. It is easy to show that $N_Z(H/h) = \varphi(z, \bar{H}, h)N_0(H/h_1)$, where z is the zenith distance of the sun at the instant of observation, $\bar{H}$ is the local altitude scale, and $\varphi(z, \bar{H}, h)$ is some function of the zenith distance, of the altitude, and of the altitude scale. For $z = 69°$ (the conditions of [25]) $\varphi = 2.8$ for 120 km and 1.6 for the exosphere. Assuming that the hydrogen atmosphere consists of only two layers with different temperatures, it was found empirically that

$$W_z = W_z^{(1)} + \beta(N_z^{(1)})\, w_z^{(2)}, \qquad (9)$$

where the indices (1) and (2) pertain to the upper (hot) and lower (cold) layers and their dependence on N(H/h) is shown in Fig. 9. The coefficient is

$$\beta = \exp[-1.5\cdot10^{-13}N_z^{(1)}(H/h)].$$

Figure 10 shows $W_{69°}$ as a function of n(H/500 km) calculated by means of this formula for 100 and 200 km at $T(\infty) = 1000$ and 1250°K. According to [25], $W_{69°}$(200 km) = 0.014 Å and $W_{69°}$(100 km) = 0.028 Å, making it possible to estimate $T(\infty)$[50]. In fact, the quantity r = N(H/100 km)/N(H/200 km) is equal to 2.6, 4.1, 8.5, and 16.4 at $T(\infty)$ = 1000, 1250, 1500, and 2000°K.

By determining $N_{69°}$(H/100 km) and $N_{69°}$(H/200 km) from Fig. 10, we obtain r = 3.2. A comparison of the calculated value with the experimental results leads to the conclusion that $T(\infty)$ = 1100°K. It should be remembered that this temperature pertains to 7 AM local time.

Both exosphere models (Johnson-Fish and Opik-Singer) have spherical symmetry and yield a value $N(H) \sim 5 \times 10^{12}$ cm^{-2} for the number of atoms of hydrogen along the line of sight. Apparently, there is still a real discrepancy by a factor 3—4 between the daytime and night time values of N(H). To be sure, the work of Bates and Patterson[47] has greatly reduced this difference. Nevertheless, it is possible to attempt to explain the observed distribution of the diffusion glow in L_α without involving multiple scattering, as was done by Brandt.

According to [51] the hydrogen is localized essentially at large distances, at least farther than 5—10 R_E, and has a noticeable asymmetrical distribution around the earth, due to the pressure of the solar wind and L_α radiation. For $R < 10\,R_E$, the Johnson-Fish model is used[41], but with one-third the density. Such an assumption does not contradict the observations of the L_α profile. In this case the 20% minimum in the antisolar point is explained by the fact that the effective distance to the scattering region, observed with a photometer with a 32° field, is $\sim 15\,R_E$. For such a distance, a greater role is assumed by the collisions between the dissipating atoms and the interplanetary protons, which, according to Chamberlain[52,53] have a temperature $\sim 2 \times 10^4$°K, an expansion rate ~18 km/sec, and a density 30 cm^{-3}. The latter figure is in good agreement with the presently assumed upper limit of the density of the interplanetary medium (see, for example, [35]). The main process in this case is

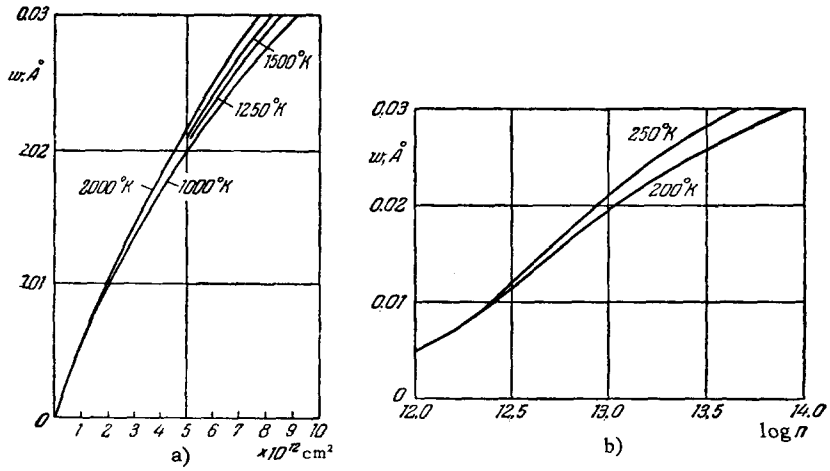

FIG. 9. a) Equivalent width of the absorption core of the L_α line (λ = 1215.7 Å) as a function of the number of the atoms along the line of sight, for four values of the temperature; b) equivalent width of the core of the L_α line for the lower layers of the atmosphere.

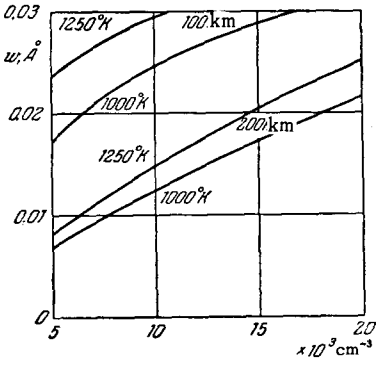

FIG. 10. Equivalent width of the absorption core of the L_α line for z = 69° at h = 100 and 200 km as a function of the hydrogen density at h = h_d. The calculation results are presented for T = 1000 and 1250°K.

charge exchange of the neutral atoms with the protons, the cross section of which is high, 8.8×10^{-17} cm^2. Then the lifetime τ_{col}, (2×10^6 sec) is much smaller than τ_{ion} (10^7 sec). Outside the sphere with radius R = 15 R_E, the number of atoms is not more than 50% of the total, while inside there are 7.5×10^{32} atoms dissipating within a time τ_{col}.

Taking into account the pressure of the L_α radiation in the line (F_{rad}), the equation of motion of the hydrogen atoms will be of the form

$$F_{rad} - \frac{m_H (v_r - w)}{\tau_{col}} = m_H \frac{dv_r}{dt}, \qquad (10)$$

where v_r is the radial velocity component and w the rate of expansion of interplanetary gas in the earth's vicinity in accord with the model of the expanding solar corona. Solution of this equation yields the time dependence of v_r, and consequently the distance covered by the hydrogen atom. The velocity will increase with increasing distance; calculation shows that it amounts to 3, 5, and 25 km/sec for 50 R_E, 100 R_E, and 4000 R_E, respectively. Consequently the density of the hydrogen in the earth's "tail" will decrease. In addition, photoionization plays a certain role and decreases the density of the neutral hydrogen. Taking these remarks into account, the density in the earth's "tail" is ~ 1 cm^{-3} at 50 R_E, decreasing to 10^{-2}–10^{-3} cm^{-3} at 10^3 R_E. This yields for N(H) a value ~ 5×10^{10} cm^{-2}, which is merely 5% of the total emission observed in L_α, half of this value "accumulating" below 125 R_E. The average deflection of the "tail" to the west is ~ 5°. Figure 11 shows the distribution of the hydrogen in accordance with this model.

3. L_α ALBEDO OF THE EARTH AND RADIATION TRANSPORT

Assuming in accordance with [13] that the radiation directed upward during the night time is the result of resonance scattering of the solar emission in the L_α line by atoms of interplanetary hydrogen, and also in agreement with the model of the earth's hydrogen "tail" proposed by Brandt [51], we can obtain the albedo as a function of the abundance of molecular oxygen and atomic hydrogen. In fact, if the optical thickness of the geocorona were to be much less than 1, then a deep minimum would be observed at the antisolar point, and the isophots would exhibit a sharp asymmetry,* contradicting the observations. At the same time, observations of the profile of the L_α line show that the optical thickness above 120 km is small.

Brandt and Chamberlain solved the problem of the night time scattering of L_α with allowance for absorption by oxygen molecules by using the Chandrasekhar scattering theory [56]. Assuming that the L_α radiation entering the atmosphere is isotropic and has a Doppler profile corresponding to a temperature T_M, they obtained for the albedo A the following expression:

$$A = \frac{2}{\sqrt{\pi}} \int_0^\infty \exp(-x_M^2) \left[1 - 2\alpha_1(\bar{\omega}_\nu)\sqrt{1-\omega_\nu^2}\right] dx_M, \qquad (11)$$

where

$$x_M = \frac{c(\nu - \nu_0)}{\nu_0 \sqrt{\frac{2kT_M}{m_p}}}, \qquad (12)$$

α_1 — first moment for the Chandrasekhar transport H-function, tabulated as a function of the frequency in [56], and ω is the albedo per cm^3, equal in turn to

*The latter is valid when the antisolar point and the zenith do not coincide.

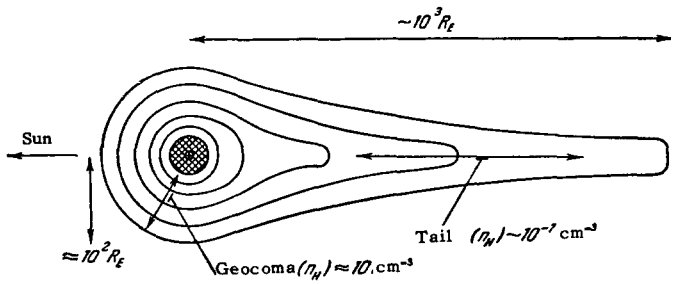

FIG. 11. Geocoma and the hydrogen "tail" of the earth in accordance with Brandt's model.

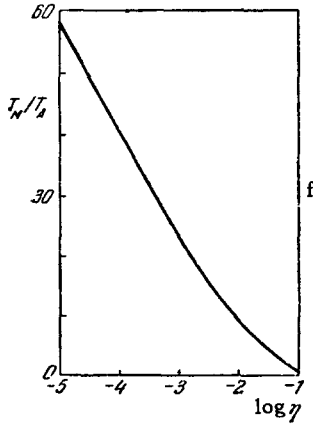

FIG. 12. Plot of η against T_M/T_A for A =0.42.

$1/(1+\eta \exp\{-x_A^2\})$. The quantity x_A corresponds to x_M, except that T_M in (11) must be replaced by the temperature of the atmosphere T_A, which is ~300°K for altitudes ~120 km and below. The quantity

$$\eta = \frac{n(O_2)\,k(O_2)}{n(H)\,k(H)}$$

characterizes the fraction of radiation absorbed per cm^3 relative to the scattered radiation [$k(O_2)$ and $k(H)$ are the absorption coefficients]. The albedo A is thus a function of two parameters, T_M/T_A and η. Using the experimental A = 0.42 we can calculate T_M/T_A as a function of η (Fig. 12). For the case $\eta < 10^{-4}$ it is also necessary to take into account the natural broadening for the atmosphere, and then A will depend also on T_A (as well as on T_M/T_A).

If we assume that the interplanetary hydrogen is not dragged by the earth, then integration over all directions gives a broad profile, which is close in shape to the Doppler profile with a certain effective temperture 6×10^4°K. Putting then $T_M/T_A = 200$ we get $\eta \sim 10^{-5}$. The transport problem for daytime observations is different in that the incident radiation comes from one direction. The value of the daytime albedo depends also on the parameter η, which determines the ratio of the abundances of the molecular oxygen to the atomic hydrogen, as well as on the temperature in the lower layers, where absorption by molecular oxygen is appreciable, i.e., on T_A. When $\eta < 10^{-4}$, which corresponds to $n(O_2)/n(H) < 3.4 \times 10^3$, the natural attenuation at temperatures ~300°K becomes appreciable. It can only be stated that $\eta < 10^{-3}$. Exact measurement of the daytime albedo rather than its upper limit could also clarify the question of the diurnal variations of the hydrogen density.

In the same paper, the authors considered the problem of first-order polarization of scattered L_α and H_α radiation, which should be ~25% in observations at 90° to the sun. The polarization should depend on the effectiveness of the collisions and on the Stark broadening, which wash out the levels with small splitting. However, measurement of the polarization of the H_α radiation is extremely difficult. The observations of this emission are in themselves a very difficult experimental task.

Brandt and Chamberlain considered scattering only as applied to the albedo problem. Thomas and Donahue [57,58] solved the transport equation in general form with account of multiple scattering in the earth's shadow. Mathematically the problem reduces to integration of the equation

$$\Omega \nabla I_\nu(\mathbf{r}, \Omega) = -k_\nu n(r)\, I_\nu(\mathbf{r}, \Omega) + j_\nu(\mathbf{r}, \Omega), \qquad (13)$$

where Ω is a unit vector, j_ν radiation coefficient, n the hydrogen density, and I_ν the intensity of radiation, which depends on the frequency of coordinates of the point of observation.

Assuming pure Doppler broadening and a spherical scattering indicatrix, we can solve this equation by successive approximations, specifying the distribution of the hydrogen in the geocorona in accordance with the model of Johnson and Fish [41]. At small optical thickness ($\tau = 0.3$), allowance for multiple scattering cannot explain the observed intensity in the antisolar point, whereas for the zenith this quantity is close to the observed value. When τ is large (~1.5) this difficulty disappears, but the intensity at the zenith and at 90° to the antisolar point increases sharply. If τ becomes even larger, then the intensity begins to decrease sharply in all directions, since the incident flux is attenuated on the daytime side even before it illuminates the shadow region. To obtain agreement with the observations it is necessary to reduce the quantity of hydrogen above $1.3\,R_E$, which decreases accordingly the contribution of the direct scattering. In order to increase the role of multiple scattering, it is desirable to shift the "center of gravity" of the hydrogen below $1.3\,R_E$. The Opik and Singer distribution model [44] with the large density gradient gives possibly better agreement in view of the foregoing. The distribution proposed by Bates and Patterson [47] for the thermosphere, in conjunction with the exosphere model of Opik and Singer, is perhaps the most acceptable. At the same time, the "geocoma" of Brandt [51] can hardly make a noticeable contribution compared with the exosphere.

It is interesting to note that the altitude distribution of the excited hydrogen atoms has a maximum in the region $1.2\,R_E$ for $\tau = 1.5$, in spite of the sharp de-

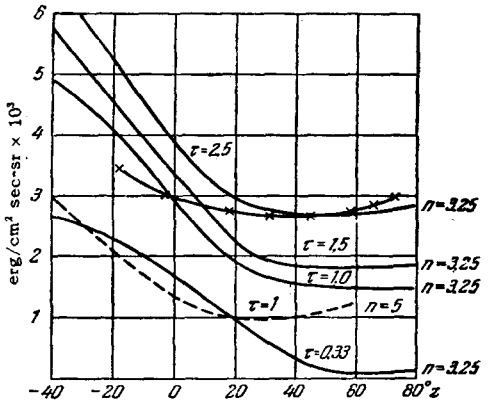

FIG. 13. The distribution of brightness in the L_α line over the sky as calculated by Thomas and Donahue[57] (× – observations).

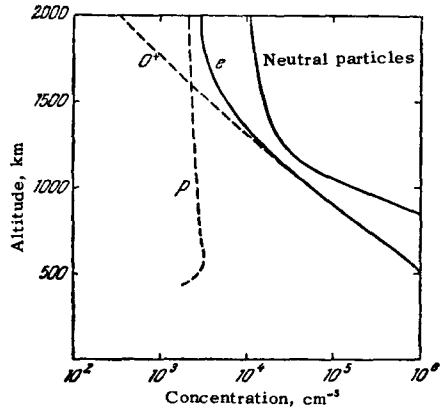

FIG. 14. Distribution of the protons, oxygen ions, electrons, and neutral atoms as a function of the altitude.

crease in the total hydrogen density.

Figure 13 shows the calculated brightness of the night sky in the L_α line as a function of the zenith distance, which is measured from the antisolar point. It is assumed that $n(H/R) = n_0(R_E/R)^n$ for the entire region of the geocorona, with the optical thickness varying from 0.33 to 2.5, n assumed equal to 3.25, and the flux in the L_α line from the sun being 6 erg/cm² sec.

Since $\tau \ll 1$ in the H_α line, the analysis of the night sky glow in this line is much simpler than in the L_α line. On the basis of his observations, Ingham[33] obtained good agreement with a model in which the density decreases somewhat more slowly than assumed by Thomas[58]. It was found empirically that

$$n\,(H/R) = 1.3\cdot 10^3 \left(\frac{R_E}{R}\right), \qquad R < 9R_E,$$

$$n\,(H/R) = 1.2\cdot 10^4 \left(\frac{R_E}{R}\right)^2, \quad 9R_E \leqslant R < 15R_E,$$

$$n\,(H/R) = 1.7\cdot 10^5 \left(\frac{R_E}{R}\right)^3, \quad 15R_E \leqslant R.$$

Such a model, unfortunately, calls for too low a density at the base of the exosphere if it is to be reconciled with the results of the observations of the absorption core of the L_α solar line.

4. EFFECTS CONNECTED WITH THE GEOCORONA

We have considered above three effects connected with the presence of the geocorona: scattering of the solar radiation in the L_α line on the night side of the earth, formation of the telluric absorption core in the solar L_α line in daytime observations of the profile of this line, and H_α emission of the night sky.

However, these are not all the problems connected with atomic hydrogen in the upper atmosphere of the earth and interplanetary space.

First, the atomic hydrogen can enter into a charge-exchange reaction with the protons of the corpuscular streams, and also with the protons captured by the earth's magnetic field.

According to Stuart[59] the lifetime of protons with energy smaller than 20 keV is determined essentially by just this process and depends only on the hydrogen concentration. A natural consequence of charge exchange will be the restoration of the earth's magnetic field to its normal value during the time of a magnetic storm caused by penetration of solar protons with energy 1—10 keV. The resultant protons with thermal or somewhat higher velocities cannot produce noticeable magnetic disturbances, and the characteristic time of this process is $\sim 10^5$ sec[60].

In addition to charge exchange with protons, charge exchange with oxygen ions is also important, since the cross section of this process is extremely large (larger than the gas-kinetic cross section), owing to the equality of the ionization potentials (the difference is only 0.02 eV, which is much less than the kinetic energy of the particles). According to Johnson[61,62] it is just this reaction that insures the equilibrium concentration of the protons in the altitude region below 700 km. Above this altitude, the proton concentration is determined more readily by the diffusion from the lower layers. There is no need for emphasizing that the role of the ionization of the dissipating hydrogen atoms by the ultraviolet radiation from the sun is negligibly small. Figure 14 shows the proton distribution in the transition region as a function of the altitude.

An analogous point of view was developed in the exceedingly interesting work of Bates and Patterson[47], which was referred to above, and is in numerical agreement with Johnson's calculations.

The electron density determined by observing whistlers and also from readings of charged-particle traps installed on space rockets agrees in order of magnitude with these calculations.

Johnson[62] analyzed the possible role of the geocorona in both vertical and horizontal heat transport from high to low latitudes. It can be shown that for the former case there is a directed downward flux of $\sim 10^{-5}$ erg/cm² sec. It is necessary to postulate here a high density of the interplanetary medium ($\sim 10^2$ cm^{-3}) at a temperature $\sim 2 \times 10^5$ °K. The latter point of view was advanced by Chapman but has presently few

supporters. An account of Parker's "solar wind" can give a quantity which is 10^2 times larger, which is still one-hundredth the observed value. Neither is the horizontal transport of heat apparently connected with the corona, since the circulation in the atmosphere is more effective.

In addition to neutral hydrogen, deuterium can also dissipate from the earth's atmosphere. It must be noted that the abundance of deuterium relative to hydrogen varies with altitude, so that the flux of dissipating atoms [see Eq. (6)] depends on the velocity B which for deuterium is equal to 1, 1.5×10^1, 8.8×10^1 and 8.2×10^2 cm/sec for T values of 1000, 1250, 1500, and 2000°K respectively, which is approximately one-hundredth that of hydrogen. Its abundance relative to hydrogen is therefore larger in the thermosphere than in the lower layers. According to calculations by Bates and Patterson [47] the relative abundance of deuterium compared with the mixing zone at an altitude of 300 km, is 5, 9, 15, and 8 times larger for T = 1000, 1250, 1500, and 2000°K, respectively. In the latter case the decrease is connected with the fact that at high temperatures the flux of the dissipating deuterium atoms increases sharply. Of course, one must not forget that this is true only if it is assumed that total mixing takes place up to 120 km.

Finally, the dissipation of helium is also of great interest. Recent experiments have disclosed the presence in the upper atmosphere of helium ions and of neutral helium, which apparently remains the main component at ~ 1500 km. In addition, twilight emission was observed in the helium line λ 10830 Å. This, however, should be the subject of a separate investigation.

It can be assumed that the main problem connected with the geocorona, namely the distribution of the neutral hydrogen and the variations that are superimposed on this distribution, will be completely solved in the nearest future. This refers primarily, of course, to diurnal variations, but it is possible that sporadic variations connected with corpuscular intrusion and heating of the atmosphere in the polar regions also exist. This leads to an increase in the rate of dissipation and to a decrease in the density of the hydrogen in the geocorona. According to Donahue [64], who used the model of Kockarts and Nicolet [65] for the thermosphere and the model of Opik and Singer for the exosphere, the density of the hydrogen at altitudes of 1000—3000 km is one order of magnitude higher at night time than during the day. The main component in this zone is helium, whose concentration reaches during the day 5×10^5 cm^{-3} at 1000 km, or practically 300 times the hydrogen concentration at this altitude. At night this difference is reduced to one-tenth (3×10^4 cm^{-3} for hydrogen and 3×10^5 cm^{-3} for helium). At approximately 1500 km the hydrogen becomes predominant at night, whereas during the day the boundary shifts to approximately 4000 km (see the appendix).

In the next few years it will be possible to map the brightness distribution in the L_α line of the night sky at different altitudes, and also to study the variation of the brightness with altitude up to several earth's radii. If the Brandt model comes close to the true distribution, such observations should be continued to several million kilometers.

It can be assumed that systematic observations in the H_α line will also help clarify the nature of the geocorona.

It is necessary to determine also the exact value of the daytime albedo in the L_α line. Further, much future promise is held out by instruments which measure directly the concentration of neutral atoms—neutral composition mass spectrometers. So far, to be sure, they have a rather low sensitivity, owing to the low efficiency of the ion source, but it can be hoped that the use of mass spectrometers with large atom-gathering area will raise their sensitivity to 10^4 cm^{-3} and perhaps better.

The last to be mentioned is the presence of hydrogen coronas in other planets, primarily Venus and Mars, although the presence of water vapor in the atmospheres of these planet has not yet been reliably established. Brandt [51] has noted that the earth's hydrogen tail, which is observable from a distance ~ 100 R_E, should have a brightness ~ 100 R, which can be readily observed. Even if the brightness of the "hydrogen tail" of Venus is 5—10 times smaller, attempts at its observation are not hopeless.

The use of optical apparatus analogous to that used in the rocket experiments but mounted on space ships sent to Mars and Venus, is also highly promising.

APPENDICES

Table I. Model of the atmosphere according to [47,49]. Most probable value T(∞) = 1100°K

T (∞), °K	h, km	T (h), °K	n (O/h)	n (O_2/h)	n (N_2/h)	ρ, g/cm³
1000	120	380	$3.4\cdot10^{10}$	$8.8\cdot10^{10}$	$4.4\cdot10^{11}$	$2.6\cdot10^{-11}$
	140	674	$9.6\cdot10^{9}$	$1.2\cdot10^{10}$	$7.4\cdot10^{10}$	$4.4\cdot10^{-12}$
	160	828	$4.8\cdot10^{9}$	$3.9\cdot10^{9}$	$2.6\cdot10^{10}$	$1.5\cdot10^{-12}$
	180	909	$2.9\cdot10^{9}$	$1.5\cdot10^{9}$	$1.1\cdot10^{10}$	$7.0\cdot10^{-13}$
	200	952	$1.9\cdot10^{9}$	$6.8\cdot10^{8}$	$5.6\cdot10^{9}$	$3.5\cdot10^{-13}$
	250	990	$7.3\cdot10^{8}$	$1.1\cdot10^{8}$	$1.1\cdot10^{9}$	$7.6\cdot10^{-14}$
	300	998	$3.0\cdot10^{8}$	$1.8\cdot10^{7}$	$2.3\cdot10^{8}$	$2.0\cdot10^{-14}$
	350	1000	$1.3\cdot10^{8}$	$3.2\cdot10^{6}$	$5.1\cdot10^{7}$	$6.0\cdot10^{-15}$
	400	1000	$5.4\cdot10^{7}$	$5.9\cdot10^{5}$	$1.2\cdot10^{7}$	$2.0\cdot10^{-15}$
	450	1000	$2.4\cdot10^{7}$	$1.1\cdot10^{5}$	$2.7\cdot10^{6}$	$7.6\cdot10^{-16}$
	500	1000	$1.0\cdot10^{7}$	$2.1\cdot10^{4}$	$6.4\cdot10^{5}$	$3.1\cdot10^{-16}$
1250	140	700	$9.3\cdot10^{9}$	$1.2\cdot10^{10}$	$7.2\cdot10^{10}$	$4.3\cdot10^{-12}$
	160	901	$4.6\cdot10^{9}$	$3.8\cdot10^{9}$	$2.5\cdot10^{10}$	$1.5\cdot10^{-12}$
	180	1028	$2.8\cdot10^{9}$	$1.6\cdot10^{9}$	$1.2\cdot10^{10}$	$7.0\cdot10^{-13}$
	200	1109	$1.8\cdot10^{9}$	$7.6\cdot10^{8}$	$6.0\cdot10^{9}$	$3.7\cdot10^{-13}$
	250	1204	$7.9\cdot10^{8}$	$1.5\cdot10^{8}$	$1.5\cdot10^{9}$	$9.7\cdot10^{-14}$
	300	1234	$3.8\cdot10^{8}$	$3.5\cdot10^{7}$	$4.1\cdot10^{8}$	$3.1\cdot10^{-14}$
	350	1245	$1.9\cdot10^{8}$	$8.8\cdot10^{6}$	$1.2\cdot10^{8}$	$1.1\cdot10^{-14}$
	400	1248	$9.5\cdot10^{7}$	$2.2\cdot10^{6}$	$3.6\cdot10^{7}$	$4.3\cdot10^{-15}$
	450	1249	$4.8\cdot10^{7}$	$5.9\cdot10^{5}$	$1.1\cdot10^{7}$	$1.8\cdot10^{-15}$
	500	1250	$2.5\cdot10^{7}$	$1.6\cdot10^{5}$	$3.5\cdot10^{6}$	$8.4\cdot10^{-16}$
1500	140	716	$9.2\cdot10^{9}$	$1.2\cdot10^{10}$	$7.1\cdot10^{10}$	$4.2\cdot10^{-12}$
	160	949	$4.5\cdot10^{9}$	$3.8\cdot10^{9}$	$2.5\cdot10^{10}$	$1.5\cdot10^{-12}$
	180	1113	$2.7\cdot10^{9}$	$1.6\cdot10^{9}$	$1.2\cdot10^{10}$	$7.0\cdot10^{-13}$
	200	1227	$1.8\cdot10^{9}$	$7.9\cdot10^{8}$	$6.2\cdot10^{9}$	$3.8\cdot10^{-13}$
	250	1385	$8.1\cdot10^{8}$	$1.8\cdot10^{8}$	$1.7\cdot10^{9}$	$1.1\cdot10^{-13}$
	300	1451	$4.2\cdot10^{8}$	$5.1\cdot10^{7}$	$5.5\cdot10^{8}$	$3.9\cdot10^{-14}$
	350	1479	$2.3\cdot10^{8}$	$1.5\cdot10^{7}$	$1.9\cdot10^{8}$	$1.6\cdot10^{-14}$
	400	1491	$1.3\cdot10^{8}$	$4.9\cdot10^{6}$	$7.0\cdot10^{7}$	$6.9\cdot10^{-15}$
	450	1496	$7.3\cdot10^{7}$	$1.6\cdot10^{6}$	$2.6\cdot10^{7}$	$3.2\cdot10^{-15}$
	500	1498	$4.2\cdot10^{7}$	$5.3\cdot10^{5}$	$1.0\cdot10^{7}$	$1.6\cdot10^{-15}$
2000	140	733	$9.0\cdot10^{9}$	$1.2\cdot10^{10}$	$7.0\cdot10^{10}$	$4.1\cdot10^{-12}$
	160	1008	$4.3\cdot10^{9}$	$3.8\cdot10^{9}$	$2.5\cdot10^{10}$	$1.5\cdot10^{-12}$
	180	1222	$2.6\cdot10^{9}$	$1.6\cdot10^{9}$	$1.2\cdot10^{10}$	$6.9\cdot10^{-13}$
	200	1389	$1.7\cdot10^{9}$	$8.3\cdot10^{8}$	$6.3\cdot10^{9}$	$3.8\cdot10^{-13}$
	250	1664	$8.1\cdot10^{8}$	$2.2\cdot10^{8}$	$1.9\cdot10^{9}$	$1.2\cdot10^{-13}$
	300	1814	$4.5\cdot10^{8}$	$7.3\cdot10^{7}$	$7.3\cdot10^{8}$	$5.0\cdot10^{-14}$
	350	1896	$2.7\cdot10^{8}$	$2.8\cdot10^{7}$	$3.1\cdot10^{8}$	$2.3\cdot10^{-14}$
	400	1941	$1.7\cdot10^{8}$	$1.1\cdot10^{7}$	$1.4\cdot10^{8}$	$1.2\cdot10^{-14}$
	450	1966	$1.1\cdot10^{8}$	$4.7\cdot10^{6}$	$6.5\cdot10^{7}$	$6.2\cdot10^{-14}$
	500	1981	$7.1\cdot10^{7}$	$2.0\cdot10^{6}$	$3.1\cdot10^{7}$	$3.5\cdot10^{-15}$

Table II. Distribution of atomic oxygen, helium, and hydrogen for temperatures 1000 and 1500°K, after [64]

h, km	T=1000° K		T=1500° K		
	n (O/h)	n (He/h)	n (H/h)	n (O/h)	n (He/h)	n (H/h)
100		$2\cdot10^{7}$	$3\cdot10^{7}$		$2\cdot10^{7}$	$3\cdot10^{7}$
200	$2\cdot10^{9}$	$1\cdot10^{7}$	$2.5\cdot10^{5}$	$2\cdot10^{9}$	$1.5\cdot10^{7}$	$7\cdot10^{4}$
500	$3\cdot10^{7}$	$1.7\cdot10^{6}$	$9\cdot10^{4}$	$1.5\cdot10^{8}$	$4\cdot10^{6}$	$9\cdot10^{3}$
1000	$8\cdot10^{3}$	$2.5\cdot10^{5}$	$3\cdot10^{4}$	$3\cdot10^{5}$	$6\cdot10^{5}$	$3\cdot10^{3}$
3000	<10	$8\cdot10^{3}$	$9\cdot10^{3}$	<10	$1\cdot10^{4}$	$1.2\cdot10^{3}$
10000		<1	$1\cdot10^{3}$			$2\cdot10^{2}$
30000			30			20

[1] S. K. Mitra, The Upper Atmosphere, 2d ed., Calcutta, 1952.

[2] J. H. Jeans, Bull. Meteor. Weather Obs. 2, 6 (1910).

[3] J. H. Jeans, Dynamical Theory of Gases, Cambridge, 1916.

[4] W. J. Humpreys, Physics of the Air, Lippincott, 1920.

[5] S. Chapman and E. A. Milne, Quart. J. Roy. Meteor. Soc. 46, 357 (1920).

[6] A. B. Meinel, Astrophys. J. 111, 207 (1950).

[7] A. B. Meinel, Astrophys. J. 111, 433 (1950).

[8] V. I. Krasovskiĭ, DAN SSSR 66, 53 (1949).

[9] I. S. Shklovskiĭ, Izvestiya, Crimean Astron. Obs. 7, 34 (1951).

[10] I. S. Shklovskiĭ, UFN 75, 351 (1961), Soviet Phys. Uspekhi 4, 812 (1962).

[11] G. M. Nikol'skiĭ, Geomagnetizm i aeronomiya 2, 3 (1962).
[12] T. A. Chubb and H. Friedman, Rev. Sci. Instr. 26, 494 (1955).
[13] Collection: "Na poroge v kosmos" (At the Threshold of Space), IL, 1960, p. 283.
[14] Collection: "Astronomicheskie nablyudeniya za predelami atmosfery" (Astronomic Observations Beyond the Atmosphere), IL, 1962, p. 80.
[15] Byram, Chubb, and Friedman, Phys. Rev. 98, 1594 (1955).
[16] Byram, Chubb, Friedman, and Kupperian, Planet and Space Sci. 1, 3 (1959).
[17] Byram, Chubb, Friedman, and Kupperian, Ann. géophys. 14, 329 (1958).
[18] Kupperian, Milligan, and Bogges, Astrophys. J. 128, 453 (1958).
[19] Byram, Chubb, and Friedman, Ultraviolet Radiation of the Sun and the Interplanetary Medium. Paper at COSPAR Symposium, Nice, 1960, (Russ. Transl., IL, 1962, p. 199).
[20] Chubb, Friedman, Kreplin, and Mange, Les spectres des Astres dans L'ultraviolet lointain, Liege, 1961, p. 437.
[21] Fastie, Crosswhite, and Markham, Ann. geophys. 17, 109 (1961).
[22] D. C. Morton, Planet and Space Sci. 9, 499 (1962).
[23] D. C. Morton and J. D. Purcell, Planet and Space Sci. 9, 455 (1962).
[24] G. M. Nikol'skiĭ, Astron. zh. 35, 657 (1958), Soviet Astronomy 2, 610 (1959).
[25] J. D. Purcell and R. Tousey, Les spectres des Astres dans L'ultraviolet lointain, Liege, 1961, p. 283.
[26] V. P. Shcheglov, op. cit. [31].
[27] J. T. Jefferies and A. T. Thomas, Astrophys. J. 129, 401 (1954).
[28] D. Morton and D. Waiding, Astroph. J. 133, 596 (1961).
[29] I. S. Shklovskiĭ, Planet and Space Science 1, 63 (1959).
[30] V. S. Prokudina, Spektral'nye elektrofotometricheskie i radiolokatsionnye issledovaniya polyarnykh siyaniĭ i nochnogo neba (Spectral Electrophotometric and Radar Investigations of Auroras and the Night Sky), AN SSSR, 1959, p. 43.
[31] Coll. "Polyarnye siyaniya i svechenie nochnogo neba (Auroras and Night Glow), No. 10, AN SSSR, 1963.
[32] G. Kvifte, J. Atmos. Terr. Phys. 16, 252 (1959).
[33] M. F. Ingham, Month. Not. Roy. Astron. Soc. 124, 523 (1962).
[34] M. Romer, Mittel Univ. Sternwarte (Bonn), 1961, p. 37.
[35] Gringauz, Kurt, Moroz, and Shklovskiĭ, Astron. zh. 37, 716 (1960), Soviet Astronomy 4, 680 (1961).
[36] W. J. Humphreys, Physics of the Air, N.Y., 1940.
[37] L. P. Granath, Phys. Rev. 34, 1045 (1929).
[38] C. W. Allen, Astrophysical Quantities (Russ. Transl.) IL, 1960, p. 145.
[39] K. Watanabe, Advances Geophys. 5, 153 (1958).
[40] D. R. Bates and M. Nicolet, J. Geophys. Res. 55, 301 (1950).
[41] F. S. Johnson and R. A. Fish, Astrophys. J. 131, 502 (1960).
[42] S. F. Singer, Phys. Fluids 2, 653 (1959).
[43] S. F. Singer and E. J. Opik, Phys. Fluids 3, 486 (1960).
[44] S. F. Singer, Planet and Space Sci. 2(4), 263 (1960).
[45] D. R. Bates, Proc. Roy. Soc. A253, 451 (1959).
[46] K. E. Grew and T. L. Ibbs, Thermal Diffusion in Gases, Cambridge, 1952.
[47] D. R. Bates and T. N. Patterson, Planet and Space Sci. 5, 257 (1961).
[48] Coll. "The Atmospheres of the Earth and Planets," G. K. Kuiper, ed., Univ. of Chicago Press, 1952.
[49] D. King-Hele and D. M. Walker, Nature 186, 928 (1960).
[50] D. R. Bates and T. N. Patterson, Planet and Space Sci. 5, 328 (1961).
[51] J. C. Brandt, Astrophys. J. 134, 394 (1961).
[52] J. W. Chamberlain, Astrophys. J. 131, 47 (1960).
[53] J. W. Chamberlain, Astrophys. J. 133, 675 (1961).
[54] A. Dalgarno, Proc. Phys. Soc. A66, 173 (1953).
[55] J. C. Brandt and W. Chamberlain, Astrophys. J. 130, 670 (1959).
[56] S. Chandrasekhar, Radiative Transfer, Oxford Univ. Press, 1950.
[57] G. E. Thomas and T. M. Donahue, Preprint (University of Pittsburgh, 1962).
[58] G. E. Thomas, Preprint (University of Pittsburgh, 1962).
[59] G. W. Stuart, Phys. Rev. Letts. 2, 417 (1959).
[60] A. J. Dessler and E. N. Parker, J. Geophys. Res. 64, 2239 (1959).
[61] F. S. Johnson, J. Geophys. Res. 65, 577 (1960).
[62] F. S. Johnson, Paper at COSPAR Symposium, Nice, 1960. (Russ. transl. in [19], p. 345.
[63] R. E. Barrington and J. Nishizaki, Canad. J. Phys. 38, 1642 (1960).
[64] T. M. Donahue, Preprint (University of Pittsburgh, Jan., 1963).
[65] G. Kockarts and M. Nicolet, Ann. géophys. 18, 269 (1962).

Translated by J. G. Adashko